This article has been accepted for publication in a future issue of this journal, but has not been fully edited. Content may change prior to final publication. Citation information: DOI 10.1109/TIA.2014.2332637, IEEE Transactions on Industry Applications

Independent Control of Two Permanent Magnet Synchronous Motors Fed by a Four-Leg Inverter

Shigeru Ito
Non Member IEEE
Sanken Electric Co., LTD.
Shimoakasaka, Ohnohara
Kawagoe, Japan
site@ms3.sanken-ele.co.jp

Takayuki Moroi
Non Member IEEE
Meiji University
Higasi-mita, Tama-ku
Kawasaki, Japan
ce21075@meiji.ac.jp

Yuji Kubo
Non Member IEEE
Meiji University
Higasi-mita, Tama-ku
Kawasaki, Japan
ce31035@meiji.ac.jp

Kouki Matsuse, Fellow IEEE
Meiji University
Higasi-mita, Tama-ku
Kawasaki, Japan
matsuse@isc.ac.jp

Kaushik Rajashekara, Fellow IEEE
The University of Texas at Dallas
800W. Campbell Rd. EC33, Richardson, TX 75080
K.Raja@utdallas.edu

***Abstract* - This paper proposes a vector control strategy for independent control of two permanent magnet synchronous motors (PMSMs) using a single four-leg inverter (4LI). An expanded two-arm modulation to obtain balanced three-phase output voltage is described. The paper also proposes a method to compensate the fluctuations in neutral point voltage of two-split capacitors in the dc link. The experimental results show that independent speed and position control of two PMSMs can be achieved using a single four leg inverter with the proposed vector control method.**

Index terms- four-leg inverter (4LI); permanent magnet synchronous motor (PMSM); two-arm modulation; neutral point potential compensation

I. INTRODUCTION

To reduce the number of switching devices and also the volume, a V-connection inverter with two legs has been proposed in the literature [1, 2, 4-7]. V-connection inverter needs two capacitors to divide phase voltage of one inverter into two portions. A single inverter can drive only one three-phase permanent magnet synchronous motor (PMSM). Therefore, two V-connection inverters are necessary to drive two PMSMs independently. An alternate way of driving two motors independently is using a four-leg inverter (4LI). Independent speed control of induction motors fed by the 4LI has been reported in [8-13]. However, little or no work has been reported on the independent control of two PMSMs using a single four leg inverter. This paper proposes in detail the independent vector control of two PMSMs fed by 4LI and techniques to compensate the fluctuation in neutral-point voltage of the two-split capacitors. The independent speed and position control of two PMSMs fed by the 4LI using vector control have several challenges. First, the pulse width modulation technique used for the three-phase voltage source inverter is not directly applicable for the 4LI because only two phases have to be modulated for each inverter. Secondly, the characteristics of speed and position drive are unstable when the voltage at the neutral point of the two capacitors deviates resulting in unbalance in capacitor voltages. In order to address these issues, this paper presents an expanded two-arm modulation technique. This technique modulates only two phases to obtain three-phase voltages required to control two motor drives. This paper also proposes a method of achieving a balanced three-phase current automatically using the vector control method [3]. The effective method for compensating fluctuations in voltages across the two capacitors is also explained. The proposed compensation method and independent control of two PMSMs fed by the 4LI with speed control are validated experimentally and the results are presented. The experimental results of position control are also presented.

II. MAIN CIRCUIT ARCHITECTURE OF FOUR-LEG INVERTER

Figure 1 shows the 4LI driving two three-phase PM motors. The 4LI consists of four switching legs and two split capacitors connected in series. The inverter legs U1 and V1 are connected to U and V phases of PMSM1, and U2 and V2 are connected to U and V phases of PMSM2. The W phase of both the motors is shared in common and connected to the neutral point of two-split capacitors. v_{UNi}, v_{VNi} and v_{WNi} are the phase voltages of the PMSMi (i=1, 2). v_{ki} (k=U, V, W) is phase voltage of motor i. v_{WO} indicates the neutral point potential of the two split capacitors. i_{Ui}, i_{Vi} and i_{Wi} are phase currents in the PMSMi and i_W is the inverter current in the common connection to the midpoint of the dc link capacitors. *E* is the DC-bus voltage and *C* is capacitance of each of the dc link capacitors. In this paper, to simplify the analysis, negative side of the DC-bus is chosen as the reference point.

III.EXPANDED TWO-ARM PWM

Since the inverters' W phase is connected to the neutral point of two-split capacitors, it is not possible to modulate voltage at this point. The 4LI has to be modulated using only U and V phases of the motor. Therefore, the conventional PWM technique used in three-phase VSI is directly not applicable for the 4LI.

This article has been accepted for publication in a future issue of this journal, but has not been fully edited. Content may change prior to final publication. Citation information: DOI 10.1109/TIA.2014.2332637, IEEE Transactions on Industry Applications

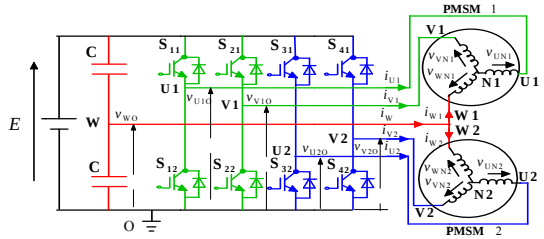

Fig.1 Power circuit of a four-leg inverter

To obtain balanced three-phase AC voltage in the 4LI, the phase difference between line voltages U-W and V-W need to be controlled to 2π/3. This is achieved by the proposed expanded two-arm modulation. Figure 2 shows the block diagram of expanded two-arm modulation for the 4LI. Reference signals for U and V phase voltages of the PMSMi are obtained by subtracting W phase voltage command from U and V phase voltage commands of the PMSMi, respectively as represented in eq. (1). Comparing reference signals with a triangular carrier signal, gate signals for the power devices can be obtained.

The reference signal for U and V phase voltages are derived as follows.

$$\begin{cases} v_{Ui}^{*} = v_{UNi}^{*} - v_{WNi}^{*} \\ v_{Vi}^{*} = v_{VNi}^{*} - v_{WNi}^{*} \end{cases} \quad (1)$$

Where, v_{kNi}^{*} is the voltage reference for phase 'k' of the motor ''. "*" represents the variable as reference value. v_{kNi}^{*} is defined as follows.

$$\begin{cases} v_{UNi}^{*} = \frac{1}{2} M_i^{*} E \sin(\omega_i^{*} t - \varphi_i^{*}) \\ v_{VNi}^{*} = \frac{1}{2} M_i^{*} E \sin(\omega_i^{*} t - \frac{2\pi}{3} - \varphi_i^{*}) \\ v_{WNi}^{*} = \frac{1}{2} M_i^{*} E \sin(\omega_i^{*} t - \frac{4\pi}{3} - \varphi_i^{*}) \end{cases} \quad (2)$$

Where, M_i^{*} and ω_i^{*} are modulation index and fundamental angular frequency for the PMSMi respectively. φ_i^{*} is the initial phase angle of the phase voltage for the PMSMi.

From eq. (2), the phase difference in each voltage waveform is controlled to be 2π/3. Substituting eq. (2) in eq. (1), three-phase line voltages are obtained. Fig.3 shows a phasor diagram for the eqs (1) and (2).

IV.UNBALANCED CURRENT COMPENSATION

The neutral point voltage of the split capacitors v_{WO} is given by the following equation.

$$v_{wo} = \frac{1}{2} E - \frac{1}{2C} \int (i_{W1} + i_{W2}) dt = \frac{1}{2} E + \Delta v_{wo} \quad (3)$$

Where, Δv_{wo} is the perturbation in voltage of v_{WO} from the ideal value of E/2.

Equation (3) shows that the voltage v_{WO} fluctuates around *E/2*. The reason for this fluctuation is due to currents drawn from the W phase of each motor which flow through the capacitors. The voltage fluctuation in v_{WO} results in unbalance of motor phase currents. The ripple component Δv_{WO} depends on the fundamental frequency of the voltage and peak value of both the motor currents.

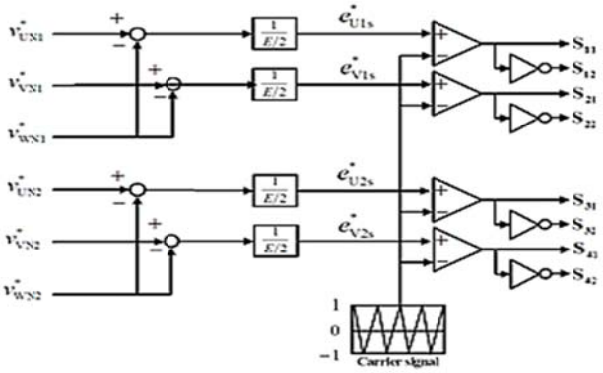

Fig.2 Block diagram of expanded two arm pulse width modulation

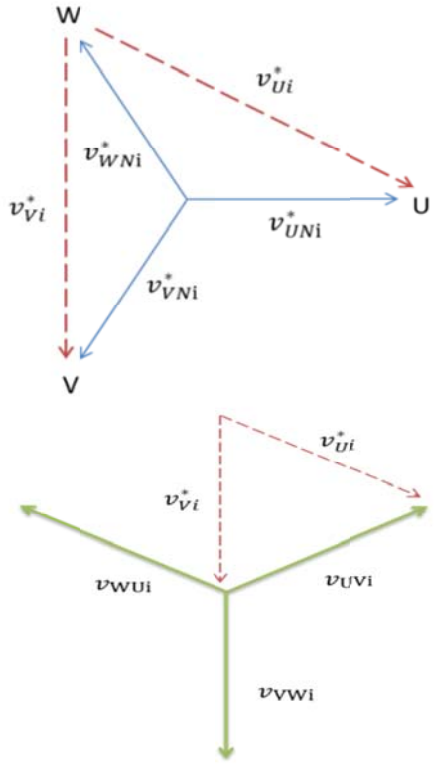

Fig.3 Voltage vector of two arm modulation

If the motors are driven at lighter load and higher speeds, the fluctuation in v_{WO} can be lower. Alternatively, using larger capacitors at the dc link can also reduce the fluctuation. However, large capacitors are undesirable because one of the advantages of going for 4LI is being the reduction in size and volume. Therefore, it is essential to consider the compensation method which balances three-phase currents without increasing the burden of additional capacitance. Since two capacitor voltages fluctuate as explained in eq. (3), the balanced three-phase current cannot be obtained under

This article has been accepted for publication in a future issue of this journal, but has not been fully edited. Content may change prior to final publication. Citation information: DOI 10.1109/TIA.2014.2332637, IEEE Transactions on Industry Applications

open-loop control such as V/f control method. In order to obtain the balanced three-phase current, fluctuation in capacitor voltage Δv_{wo} must be added to the U, V phase terminal voltage, v_{UiO}, v_{ViO} respectively such that

$$\begin{cases} v_{UiO} = v_{UNi}{}^{*} - v_{WNi}{}^{*} + \Delta v_{wo} \\ v_{ViO} = v_{VNi}{}^{*} - v_{WNi}{}^{*} + \Delta v_{wo} \end{cases} \quad (4)$$

However, in vector control, reference values to achieve balanced three-phase currents are automatically obtained because three-phase currents are calculated from d and q axis currents.

V. NEUTRAL POINT POTENTIAL COMPENSATION OF TWO-SPLIT CAPACITORS

The voltage drift at the neutral point of two capacitors, v_{WO} is observed during the starting of motors. As a result, the capacitor voltages are not equally balanced to a value E/2. The drift causes the reduction of inverter DC-bus voltage utility factor. Hence, v_{WO} must be maintained to E/2 preventing the drift. The authors in [5] analyzed the drift phenomenon of the four switch inverter controlled using space vector technique. They have presented a compensation method to eliminate the unbalance in capacitor voltage and validated the method with experimental results.

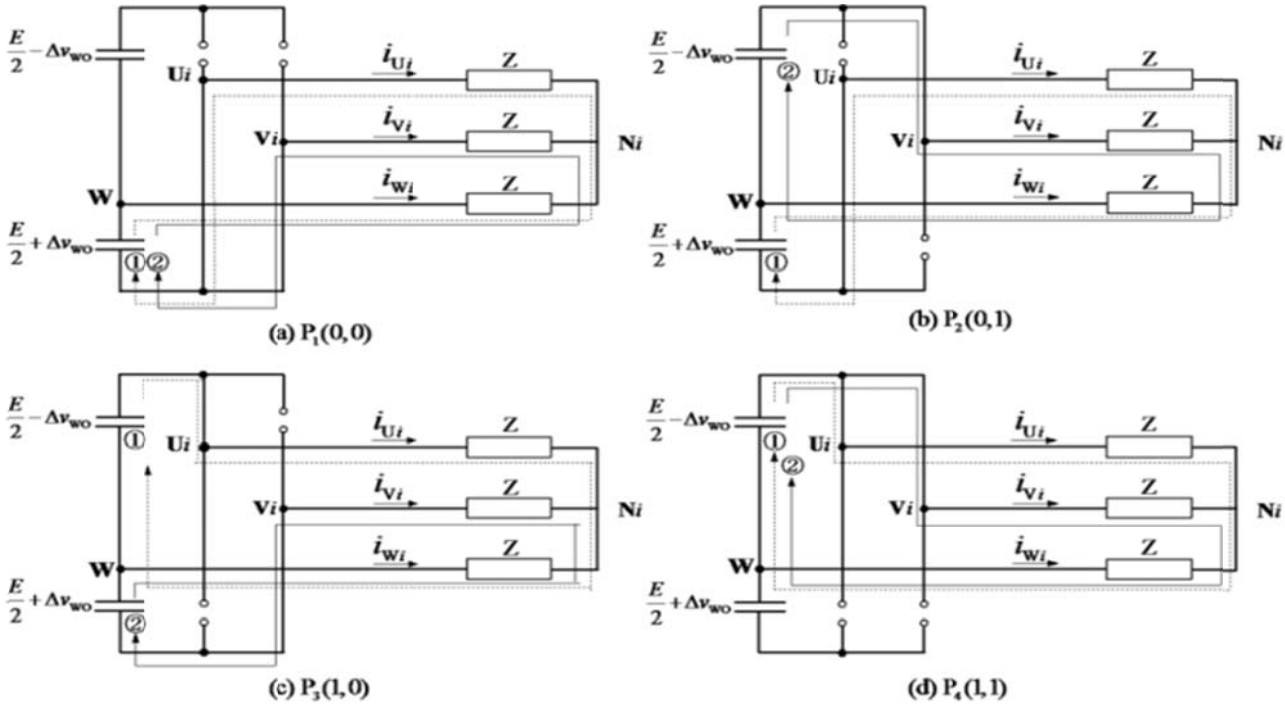

Fig.4 Current paths during each switching mode

The authors conducted circuit analysis of each switching mode of the 4LI to analyze compensation method for voltage at neutral point. Since the two motors are controlled independently, the circuit analysis for only one of the motors has been presented in this paper. Fig.4 shows the direction of current paths during each switching mode; $P_{i1}(0,0)$, $P_{i2}(0,1)$, $P_{i3}(1,0)$, $P_{i4}(1,1)$. It is defined as "1" in the parenthesis when the upper switch of each phase is turned on, and as "0" when the upper switch is off.

In mode $P_{i1}(0,0)$, eq. (5) obtained from Fig.4 (a) as

$$\begin{cases} Zi_{Wi} - Zi_{Ui} = \frac{1}{2}E + \Delta v_{wo} \\ Zi_{Wi} - Zi_{Vi} = \frac{1}{2}E + \Delta v_{wo} \\ i_{Ui} + i_{Vi} + i_{Wi} = 0 \end{cases} \quad (5)$$

Eq. (5) can be rewritten as

$$\begin{cases} Zi_{Ui} = -\frac{1}{6}E - \frac{1}{3}\Delta v_{wo} \\ Zi_{Vi} = -\frac{1}{6}E - \frac{1}{3}\Delta v_{wo} \\ Zi_{Wi} = \frac{1}{3}E + \frac{2}{3}\Delta v_{wo} \end{cases} \quad (6)$$

From figures 4(b) $P_{i2}(0,1)$, 4(c)$P_{i3}(1,0)$, and 4(d)$P_{i4}(1,1)$, the next set of equations can be obtained.

This article has been accepted for publication in a future issue of this journal, but has not been fully edited. Content may change prior to final publication. Citation information: DOI 10.1109/TIA.2014.2332637, IEEE Transactions on Industry Applications

$$\begin{cases} \mathrm{Zi_{Ui}} = -\frac{1}{2}\mathrm{E} - \frac{1}{3}\Delta \mathrm{v_{wo}} \\ \mathrm{Zi_{Vi}} = \frac{1}{2}\mathrm{E} - \frac{1}{3}\Delta \mathrm{v_{wo}} \\ \mathrm{Zi_{Wi}} = \frac{2}{3}\Delta \mathrm{v_{wo}} \end{cases} \quad (7)$$

$$\begin{cases} \mathrm{Zi_{Ui}} = \frac{1}{2}\mathrm{E} - \frac{1}{3}\Delta \mathrm{v_{wo}} \\ \mathrm{Zi_{Vi}} = \frac{1}{2}\mathrm{E} - \frac{1}{3}\Delta \mathrm{v_{wo}} \\ \mathrm{Zi_{Wi}} = \frac{2}{3}\Delta \mathrm{v_{wo}} \end{cases} \quad (8)$$

$$\begin{cases} \mathrm{Zi_{Ui}} = \frac{1}{6}\mathrm{E} - \frac{1}{3}\Delta \mathrm{v_{wo}} \\ \mathrm{Zi_{Vi}} = \frac{1}{6}\mathrm{E} - \frac{1}{3}\Delta \mathrm{v_{wo}} \\ \mathrm{Zi_{Wi}} = -\frac{1}{3}\mathrm{E} + \frac{2}{3}\Delta \mathrm{v_{wo}} \end{cases} \quad (9)$$

Equations (6)-(9) show relation between each phase voltage and $\Delta \mathrm{V}_{wo}$. From these equations, we analyzed the relation of the inverter phase voltage and drift phenomenon of the neutral point potential by using space vector representation.

Each Voltage vectors $\mathrm{P_{i1}}(0,0)$, $\mathrm{P_{i2}}(0,1)$, $\mathrm{P_{i3}}(1,0)$, $\mathrm{P_{i4}}(1,1)$ are expressed $\mathbf{V}_{i1}$, $\mathbf{V}_{i2}$, $\mathbf{V}_{i3}$, $\mathbf{V}_{i4}$ respectively.

$\mathbf{V}_{i1}$ expressed as:

$$V_{i1} = \frac{2}{3}\left(Zi_{Ui} + \mathrm{Zi}_{Vi}e^{j(\frac{2}{3}\pi)} + Zi_{Wi}e^{j(\frac{4}{3}\pi)}\right) \quad (10)$$

Substituting eq. (6) into (10) and then

$$V_{i1} = \left(-\frac{1}{6} - j\frac{1}{2\sqrt{3}}\right)E + \frac{2}{3}\Delta v_{wo}e^{j(\frac{4}{3}\pi)}$$

Further simplifying,

$$\mathrm{Vi1} = \left(-\frac{1}{6} - j\frac{1}{2\sqrt{3}}\right)E + \Delta \mathrm{V}_{wo} \quad (11)$$

where

$$\Delta \mathrm{V}_{wo} = \frac{2}{3}\Delta v_{wo}e^{j(\frac{4}{3}\pi)}$$

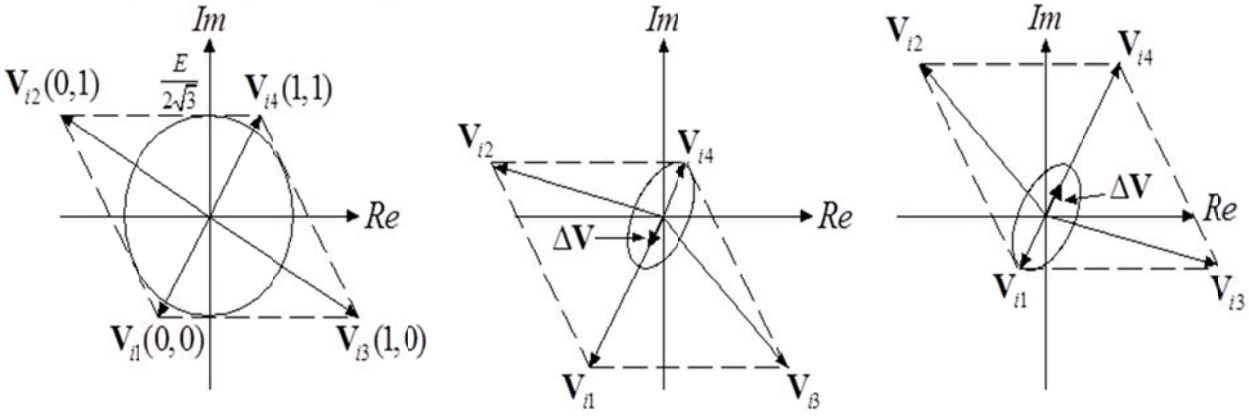

(a) $\Delta \mathrm{V}_{wo} = 0$ (b) $\Delta \mathrm{V}_{wo} > 0$ (c) $\Delta \mathrm{V}_{wo} < 0$

Fig.5 Space vector of four-leg inverter

Similarly, $\mathrm{V_{i2}}$, $\mathbf{V}_{i3}$, $\mathbf{V}_{i4}$ are also written as:

$$V_{i2} = \left(-\frac{1}{2} + j\frac{1}{2\sqrt{3}}\right)E + \Delta \mathrm{V}_{wo} \quad (12)$$

$$V_{i3} = \left(\frac{1}{2} - j\frac{1}{2\sqrt{3}}\right)E + \Delta \mathrm{V}_{wo} \quad (13)$$

$$V_{i4} = \left(\frac{1}{6} + j\frac{1}{2\sqrt{3}}\right)E + \Delta \mathrm{V}_{wo} \quad (14)$$

From these equations, it is clear that the $\Delta \mathrm{V}_{wo}$ influences all the switching modes.

Figure 5 shows the space vector for the 4LI. In Fig. 5, case (a) shows $\Delta \mathrm{V}_{wo} = 0$. $\mathrm{V}_{wo}$is maintained to be E/2 from equation (3). If $\Delta \mathrm{V}_{wo}$ is positive or negative, the parallelogram shifts as shown in Fig. 5(b) or Fig. 5(c), and the voltage range that can be utilized decreases. The term that causes the voltage drift needs to be compensated. Figure.6 shows vector diagram of $\Delta \mathrm{V}_{wo}$, $\mathrm{V_{Ui}}$ and $\mathrm{V_{Vi}}$. From Fig.6, $\Delta \mathrm{V}_{wo}$ is compensated by adding $\Delta \mathrm{V}_{wo}$ which is divided among U and V vectors. $\Delta \mathbf{V}_{wo}$ is expressed as:

$$\begin{aligned} \Delta \mathbf{V}_{wo} &= \mathrm{sgn}(\Delta \mathbf{V}_{wo})\frac{|\Delta \mathbf{V}_{wo}|}{\sqrt{3}}\frac{\mathrm{V}_{Ui}}{|\mathbf{V}_{Ui}|} + \mathrm{sgn}(\Delta \mathbf{V}_{wo})\frac{|\Delta \mathbf{V}_{wo}|}{\sqrt{3}}\frac{\mathrm{V}_{Vi}}{|\mathbf{V}_{Vi}|} \\ &= \frac{2\Delta \mathrm{V}_{wo}}{3\sqrt{3}}\frac{\mathrm{V}_{Ui}}{|\mathbf{V}_{Ui}|} + \frac{2\Delta \mathrm{V}_{wo}}{3\sqrt{3}}\frac{\mathrm{V}_{Vi}}{|\mathbf{V}_{Vi}|} \\ &= \frac{2\Delta \mathrm{V}_{wo}}{3\sqrt{3}}\mathrm{e}^{\mathrm{j}\frac{\pi}{6}} + \frac{2\Delta \mathrm{V}_{wo}}{3\sqrt{3}}\mathrm{e}^{\mathrm{j}\frac{\pi}{2}} \end{aligned} \quad (15)$$

Where, sgn () represents change of sign.

This article has been accepted for publication in a future issue of this journal, but has not been fully edited. Content may change prior to final publication. Citation information: DOI 10.1109/TIA.2014.2332637, IEEE Transactions on Industry Applications

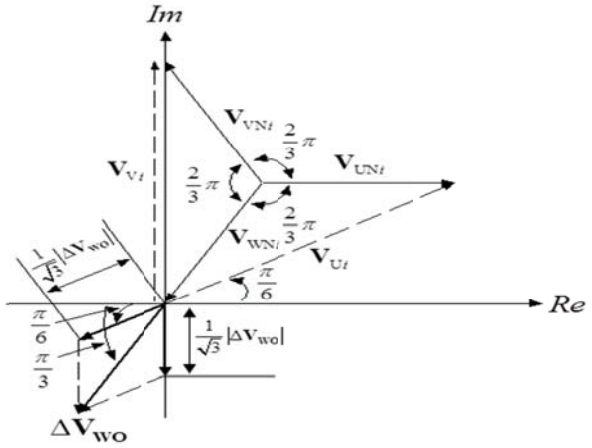

Fig.6 Space voltage vector (vector diagram of ΔV_{wo}, V_{Ui} and V_{Vi})

From eq. (15), compensation terms which are added to U or V phase voltage command are given by,

$$\begin{cases} \delta v_{Ui} = -\dfrac{2}{3\sqrt{3}}\Delta \mathrm{V}_{wo} \\ \delta v_{Vi} = -\dfrac{2}{3\sqrt{3}}\Delta \mathrm{V}_{wo} \end{cases} \tag{16}$$

For vector control method, even if the compensation terms are added to the reference signals of U and V phases prior to the comparison with the carrier signal, it does not improve the performance because the response of Automatic Current Regulator (ACR) in vector control system is very fast. Therefore, in order to use the compensation terms in eq. (16), it must be added before ACR, not after ACR. Hence, it is necessary to transform eq. (16) into d and q axes coordinates, and compensate for the d and q axes currents. In 4LI, transformation from d and q reference voltages to U and V phase sinusoidal reference voltage signals are given by,

$$\begin{aligned} \begin{bmatrix} v_{UiO} \\ v_{ViO} \end{bmatrix} &= \sqrt{\frac{2}{3}} \begin{bmatrix} 1 & 0 & -1 \\ 0 & 1 & -1 \end{bmatrix} \begin{bmatrix} \cos\theta & -\sin\theta \\ \cos\left(\theta - \frac{2}{3}\pi\right) & -\sin\left(\theta - \frac{2}{3}\pi\right) \\ \cos\left(\theta - \frac{4}{3}\pi\right) & -\sin\left(\theta - \frac{4}{3}\pi\right) \end{bmatrix} \begin{bmatrix} v_d \\ v_q \end{bmatrix} \\ &= \sqrt{2} \begin{bmatrix} \cos\left(\theta - \frac{\pi}{6}\right) & -\sin\left(\theta - \frac{\pi}{6}\right) \\ \sin\theta & \cos\theta \end{bmatrix} \begin{bmatrix} v_d \\ v_q \end{bmatrix} \end{aligned} \tag{17}$$

Also, inverse transformation of (17) is obtained as

$$\begin{bmatrix} v_d \\ v_q \end{bmatrix} = \sqrt{\frac{2}{3}} \begin{bmatrix} \cos\theta & \sin\left(\theta - \frac{\pi}{6}\right) \\ -\sin\theta & \cos\left(\theta - \frac{\pi}{6}\right) \end{bmatrix} \begin{bmatrix} v_{UiO} \\ v_{ViO} \end{bmatrix} \tag{18}$$

Substituting δv_{UiO}, δv_{ViO} of eq. (16) for v_{UiO}, v_{ViO}, it follows that

$$\begin{bmatrix} \delta v_{di} \\ \delta v_{qi} \end{bmatrix} \sqrt{\frac{2}{3}} \begin{bmatrix} \cos\theta & \sin\left(\theta - \frac{\pi}{6}\right) \\ -\sin\theta & \cos\left(\theta - \frac{\pi}{6}\right) \end{bmatrix} \begin{bmatrix} -\frac{2}{3\sqrt{3}}\Delta v_{wo} \\ -\frac{2}{3\sqrt{3}}\Delta v_{wo} \end{bmatrix} \tag{19}$$

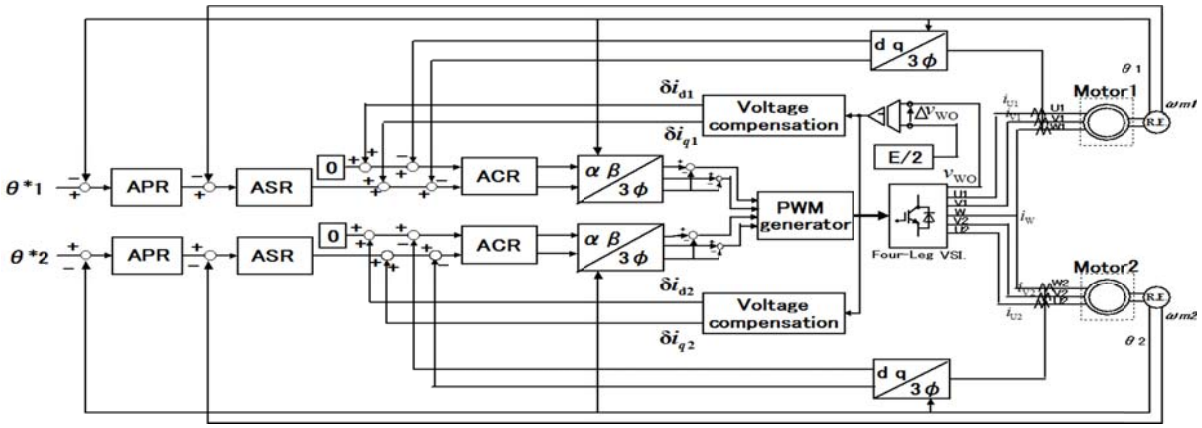

Fig.7 Block diagram of the vector control with drift voltage compensation

By diving eq. (19) by the impedance of stator winding, R+Ls; d and q axes current compensation terms δi_{di}, δi_{qi} can be obtained. The d and q axes current commands in the 4LI are obtained by adding the current compensation terms δi_{di}, δi_{qi} to the standard d and q axes current references obtained from vector control. By controlling the difference between the commands and the actual current values with Proportional and Integral (PI) controller, the drift in neutral point voltage fluctuations can be restricted.

Figure 7 shows block diagram of vector control with drift compensation. ACR and Automatic Speed Regulator (ASR) are PI controllers whereas Automatic Position Regulator (APR) is P controller.

In this study, the d and q axis proportional gains of ACR are 9.4488[V/A] and 9.8397[V/A] respectively, the d and q axis integral gains of ACR are 1743.0[V・s/A] and 1812.5[V・s/A] respectively, the proportional and integral gains of ASR are 0.30170[A/rpm] and 21.333[A・s/rpm] respectively, and the proportional gain of APR is 2.1213[rpm/rad].

VI EXPERIMENTAL RESULTS

A) Experimental system

In order to demonstrate independent control of two PMSM

This article has been accepted for publication in a future issue of this journal, but has not been fully edited. Content may change prior to final publication. Citation information: DOI 10.1109/TIA.2014.2332637, IEEE Transactions on Industry Applications

drives and the usefulness of the compensation method for the drift phenomenon, a 4LI experimental prototype has been developed in the laboratory. The system configuration of the prototype is shown in Figure 8. The main circuit consists of four IGBT-modules and two-split capacitors. The control system was based on PE-Expert3, which is a DSP based digital control system that also has an Analog-Digital (AD) Converter, digital input-output and PWM functions. The vector control algorithm is implemented by loading the program from a host computer to the DSP residing in the PE-Expert3. Figure 9 depicts a photo of experimental prototype. Table 1 provides the ratings and parameters of two identical PMSMs used in the experiment. In this experiment, in order to demonstrate independent driving of both PMSMs, the direction of rotation reference signal for PMSM1 and PMSM2 are given in opposite direction to each other. The dc bus voltage to the inverter was set at 282V and the switching frequency was 10kHz.

B) *Experimental results for Independent speed control*

Both the PMSMs were operated at half the rated load. The speed reference input to PMSM1 was changed from 250[rpm] (0-3[sec]) to 500[rpm] (3-5[sec]). The speed reference to PMSM2 was changed to accelerate from zero speed to 400 [rpm] in the reverse rotation in 2.0 seconds. Figure 10 and 11 show the rotor speed of both the PMSMs. As can be seen from these figures, two PMSMs are independently driven by the 4LI.

Figures 12 and 13 show the current waveforms of the PMSMs during steady state condition. In order to verify the reason for current distortion, the system was simulated and Figure14 shows the results of current waveforms of three phase voltage inverter at constant speed. The speed reference to PMSM was 500[rpm]. Current distortion was also observed in the simulation results. Therefore, the current distortion that was observed in the experimental results was not due to the 4 LI configuration. Figure 15 shows the voltage at neutral point with compensation. The voltage drift in v_{WO} is observed during acceleration and change in speed reference, but it is balanced in steady state conditions. Hence, it is possible to drive two PMSMs without any stability problems. The DC bus voltage was also observed to study the effect of drift in the neutral point voltage. It was observed that the dc voltage was steady and is not affected by any drift in the neutral point voltage.

C) Independent position control – experimental results

Figures 16 and 17 show the rotor position of the PMSMs when both PMSMs are driven under no load condition. A step input of 5π [rad] was given to the rotor position of PMSM1 and -3π [rad] to PMSM2 as shown by the red lines. As can be seen from these figures, there is no overshoot and each motor stops at the respective rotor position command independently. In Figures 18 and 19 are shown the three-phase current waveforms of the PMSMs. Figures 20 and 21 show the rotor position of the PMSMs for the same reference signals, where the proportional gain is twice to that of figures 18 and 19. Hence the, rotor angles reach the reference value faster than that in figures 18 and 19.

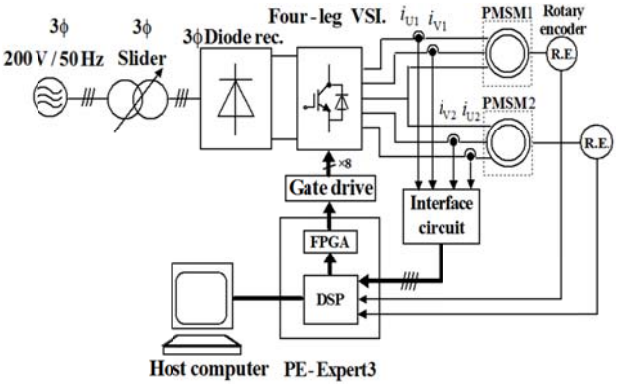

Fig.8 System block diagram of the experimental unit

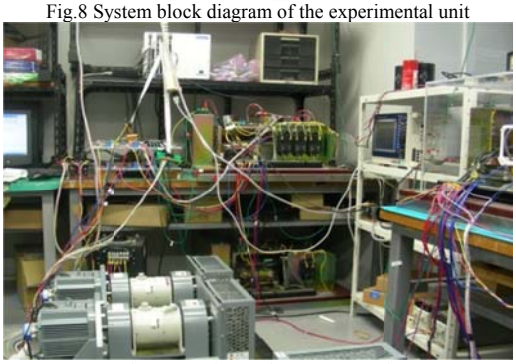

Fig.9 Experimental Prototype Unit

TABLE I Rating and parameters of tested permanent magnet synchronous motors

Rated Output	0.75 kw
The Number of Poles	12
Rated Voltage	116 Vrms
Rated Current	4.5 A
Rated Frequency	120 Hz
Rated Speed	1200 rpm
Stator Resistance	0.36 Ω
d-axis Inductance	2.76 mH
q-axis Inductance	2.87 mH
Inertia(PMSM + Load)	12.8 $mkgm^2$

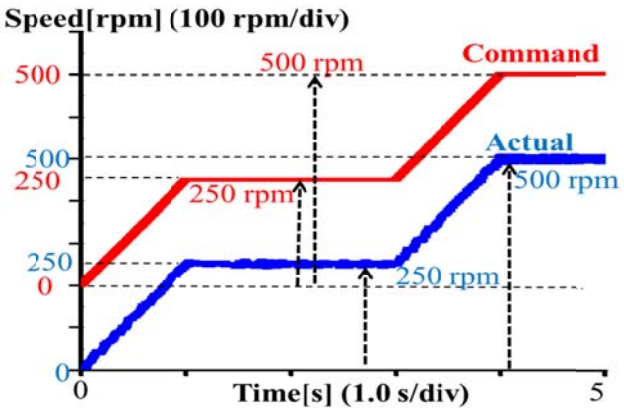

Fig.10 Speed response of PMSM1

This article has been accepted for publication in a future issue of this journal, but has not been fully edited. Content may change prior to final publication. Citation information: DOI 10.1109/TIA.2014.2332637, IEEE Transactions on Industry Applications

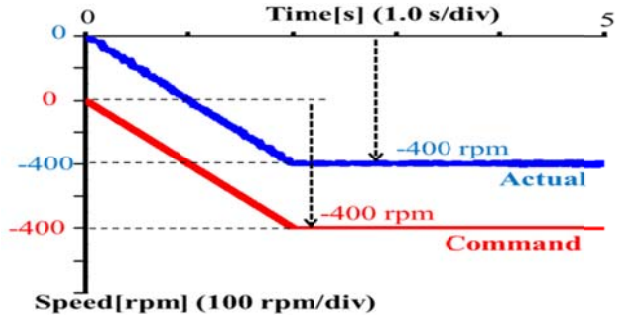

Fig.11 Speed response of PMSM2

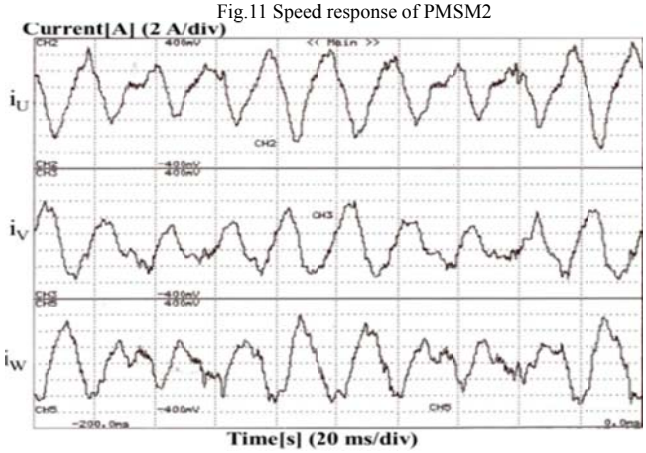

Fig. 12 Three-phase current waveforms of the PMSM1

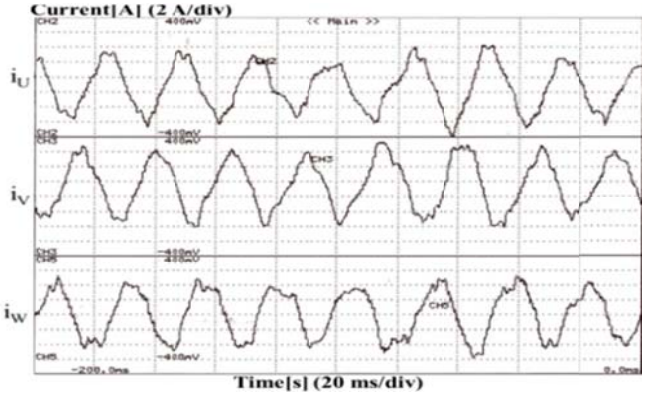

Fig.13 Three-phase current waveforms of the PMSM2

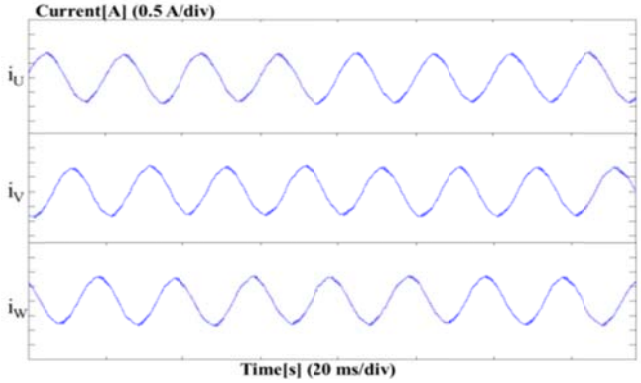

Fig.14 Current waveforms VSI in simulation result

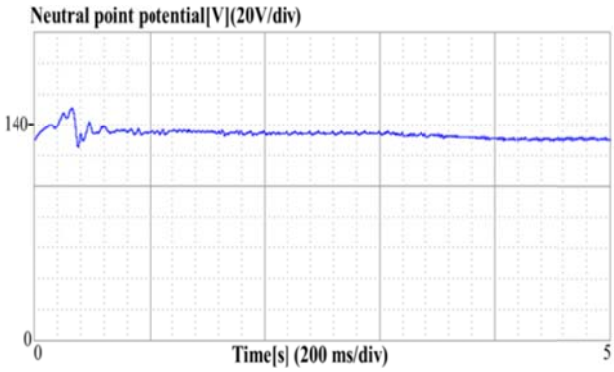

Fig.15 Neutral point potential of two capacitors in experimental result

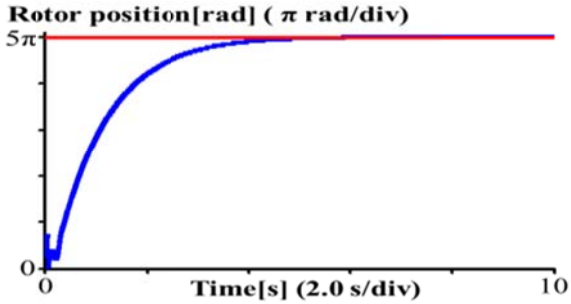

Fig.16 Rotor angle of the PMSM1

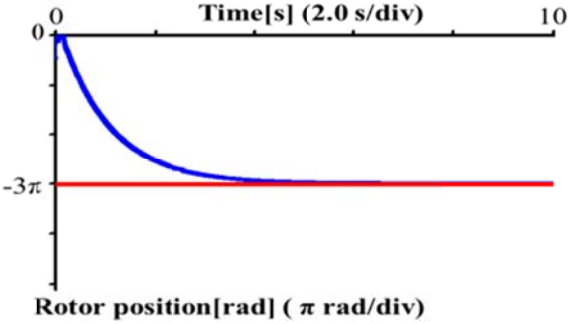

Fig.17 Rotor angle of the PMSM2

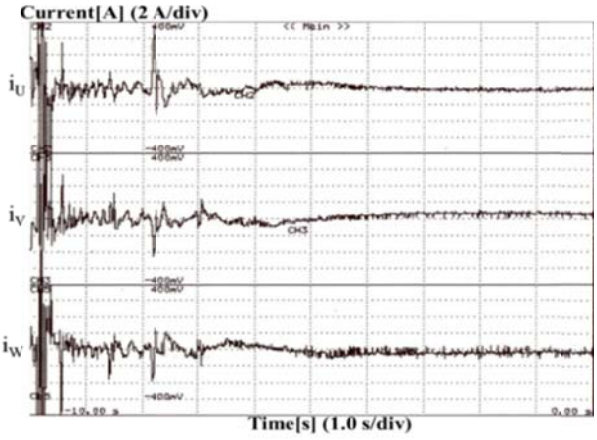

Fig.18 The three-phase current waveforms of the PMSM1

This article has been accepted for publication in a future issue of this journal, but has not been fully edited. Content may change prior to final publication. Citation information: DOI 10.1109/TIA.2014.2332637, IEEE Transactions on Industry Applications

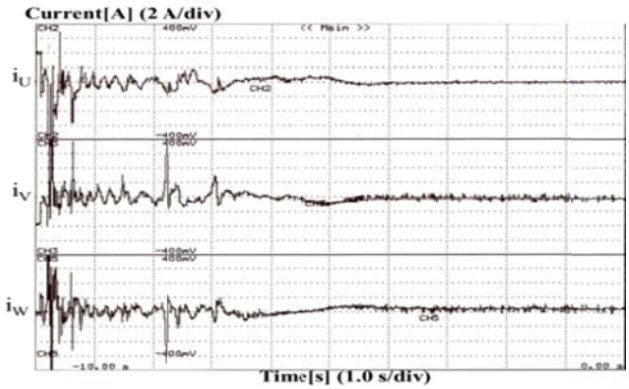

Fig.19 Three-phase current waveforms of the PMSM2

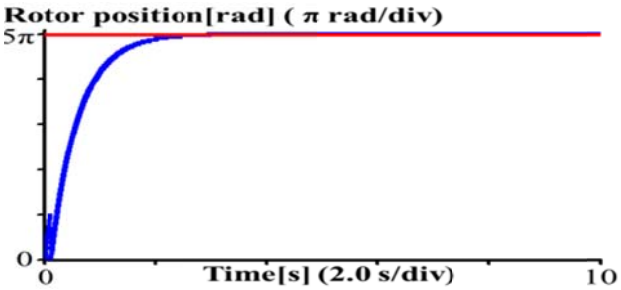

Fig.20 Rotor angle of the PMSM1 in twice proportional gain

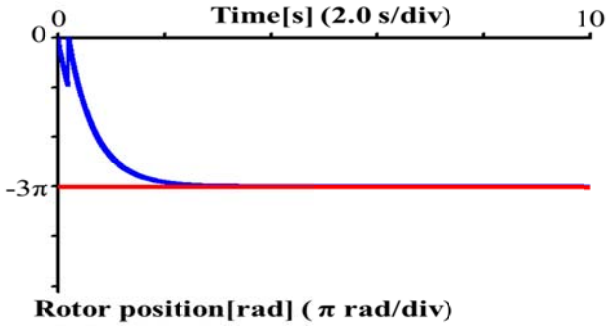

Fig.21 Rotor angle of the PMSM2 in twice proportional gain

VII. CONCLUSION

This paper presents an independent vector control strategy for controlling two PMSMs drives fed by a single four-leg inverter. The detailed block diagram of the system with voltage drift compensation is also explained. The effectiveness of the proposed method to compensate for the fluctuation in the neutral point voltage of the two split capacitors has been presented. In addition, the independent drive characteristics of two PMSMs fed by the four-leg inverter are demonstrated by the experimental results. These experimental results also validate the proposed compensation method. The results show that independent speed and position control of two PMSMs can be realized using a single four-leg inverter.

REFERENCES

[1] C. B. Jacobina, E. R. C. da Silva, A. M. N.Lima and R. L. A. Riberio, "Vector and Scalar Control of a Four Switch Three Phase Inverter", in *Proc. IEEE-IAS Annu. Meeting*, 1995. pp. 2422-2429.

[2] F. Blaabjerg, D.O. Neacsu and J.K. Pedersen, "Adaptive SVM to Compensate DC-Link Voltage Ripple for Four-switch Three-phase Voltage-Source Inverters", *IEEE Trans. Power Electon* vol. 14, no. 4, July, 1999, pp. 743-752.

[3] M.Yamato and Y.Sato, "An Investigatation of A Control Method for Fault-Mode Inverters to Drive Induction Motors", IEEE Journal of Transactions 2003, 123(12),pp. 1430-1437.

[4] M. B. de R. correa, C.B. jacobina, E. R. C. da Silva and A. M. N. Lima, "A General PWM Strategy for Four-Switch Three-Phase Inverters", *IEEE Trans. Power Electon* vol. 21, no. 6, November, 2006, pp. 1618-1627.

[5] J. Kim, J. Hong and K, Nam, "A Current Distortion Compensation Scheme for Four-Switch Inverters", *IEEE Trans. Power Electon* vol. 24, no. 4, April, 2009, pp. 1032-1040.

[6] T. D. Nguyen, H. M. Nguyen and H. H. Lee, "An Adaptive Carrier-Based PWM Method for Four-Switch Three- Phase Inverter", IEEE International symposium on Industrial Electronics, July 5-8, 2009, pp. 1552-1557.

[7] Jaehong Kim, Jinseok Hong, and Kwanghee Nam, "A Current Distortion Compensation Scheme for Four-Switch Inverters", *IEEE TRANSACTIONS ON POWER ERECTRONICS, VOL. 24, NO. 4, APRIL* 2009

[8] K.Oka and K.Matsuse, "A Performance Analysis of a Four-Leg Inverter in Two AC Motor Drives with Independent Vector Control", *TRANSACTIONS ON ELECTRONICAL AND ELECTRONIC ENGINEERING IEEJ Trans* 104-107, 2006, 1

[9] Y.Katagiri, N.Kezuka, H.tanaka, K.Matsuse, ''Performance of Independent two Induction Motor Drives Fed by a Four-Leg Inverter with vector control method'', IEEE IAS Annual Meeting, 2011-IACC-160,2011.

[10] K.Matsuse N.Kezuka K.Oka, "Characteristics of Independent Two Induction Motor Drives Fed by a Four-Leg Inverter", IEEE Trans. Industry Applications, Vol.47, NO.5, Sep./Oct. 2011, pp.2125-2134.

[11] Y.Katagiri,N.Kezuka, H.tanaka, K.Matsuse, "Independent Two Induction Motor Drives with Vector Control Method Fed by a Four-Leg Inverter", 2011 International Conference on Electrical Machines and Systems, CD-ROM, August, 2011.

[12] H.Tanaka,S.Saito, K.Matsuse, "Improved Performance of Independent Two Induction Motor Drives fed by a Four-Leg Inverter with Vector Control Method", 2012 international Conference on Electrical Machines and Systems, CD-ROM,6p,October 2012.

[13] H.Tanaka, S.Saito, K.Matsuse, "Independent vector control of Two Induction Motor Drives Fed by a Four-Leg Inverter with compensation method of capacitor voltage", 2012 IEEE Industry Applications Society Annual Meeting, 2012-IACC-184,October 2012.